

Modeling Multi-User WLANs under Closed Loop Traffic

Peshal Nayak, *Member, IEEE*, Michele Garetto, *Member, IEEE*, and Edward W. Knightly, *Fellow, IEEE*

Abstract—In this paper we present the first cross-layer analysis of wireless LANs operating under downlink multi-user MIMO (MU-MIMO), considering the fundamental role played by closed-loop (TCP) traffic. In particular, we consider a scenario in which the access point transmits on the downlink via MU-MIMO, whereas stations must employ single-user transmissions on the uplink, as is the case in IEEE 802.11ac. With the help of analytical models built for the different regimes that can occur in the considered system, we identify and explain crucial performance anomalies that can result in very low throughput in some scenarios, completely offsetting the theoretical gains achievable by MU-MIMO. We discuss solutions to mitigate the risk of this performance degradation and alternative uplink strategies allowing WLANs to approach their maximum theoretical capacity under MU-MIMO.

Index Terms—Wireless LAN, multi-user MIMO, TCP, cross-layer analysis.

I. INTRODUCTION

DOWNLINK multi-user MIMO (DL MU-MIMO) is a promising physical-layer technology to boost the capacity of wireless LANs by transmitting data streams to multiple stations (STAs) concurrently, thus scaling up the achievable data rate by a factor equal to the number of antennas on the Access Point (AP). This approach is different from traditional single-user (SU) networks where only one STA gets served at a time. With inclusion in the IEEE 802.11ac standard [1], [2], DL MU-MIMO has moved from theoretical research into the real world.

In this paper, we show that DL MU-MIMO alone, without UL MU-MIMO, does not necessarily correspond to an equivalent gain in terms of throughput perceived by users at the transport layer, even if the vast majority of bytes are transmitted in the downlink direction, e.g., via download of large files via TCP. Specifically, severe performance degradation can occur, in some scenarios, when DL MU-MIMO is coupled with a single-user uplink under closed-loop traffic such as that generated by TCP, which still carries more than 80% [3], [4], [5] of Internet traffic today. In particular, we show that a key performance factor is the amount of frame aggregation

performed during each transmission in the downlink or in the uplink.

Our work provides the following contributions: (i) we present, to the best of our knowledge, the first cross-layer performance evaluation study of MU-MIMO under closed-loop (TCP) traffic; (ii) we develop novel analytical techniques to compute the throughput of a WLAN operating under downlink MU-MIMO, and the standard channel access mechanism of 802.11; (iii) with the help of our models, we identify the fundamental reasons that can lead to poor performance and show the crucial role played by frame aggregation, as well as the intrinsic limitations due to suboptimal multiplexing gain resulting from random channel contention; (iv) we discuss different uplink strategies that can overcome the above limitations and approach the maximum theoretical performance.

The rest of the paper is organized as follows. In Sec. II we present the network scenario considered in our work, including the necessary background on DL MU-MIMO. In Sec. III we describe our model of the considered system, and a simple high-level characterization of the different regimes that can occur. Detailed analytical models are developed in Sec. IV for the most significant cases, and validated by simulation. In Sec. V we compare different uplink strategies from a system-design perspective while in Sec. VI we study the behavior of the system when we deviate from our modeling assumptions. We discuss related work in Sec. VII and conclude in Sec. VIII.

II. NETWORK SCENARIO

A. Cross-layer Setup

To investigate the performance of DL MU-MIMO under closed-loop traffic, we consider a simple network scenario and adopt some simplifying assumptions to analyze it. We emphasize that our goal is not to develop a comprehensive model to predict TCP throughput over MU-MIMO WLANs under very general and realistic conditions, but to identify crucial performance factors that can offset the gains achievable by MU-MIMO. Such factors, which are more easily understood and quantitatively analyzed in a simple (but not unrealistic) scenario, are expected to affect likewise the performance of MU-MIMO WLANs in more realistic and complex conditions.¹

We consider the network scenario illustrated in Fig. 1. A set of users (or stations²) attached to a wireless LAN establish

Manuscript received XX; revised YY; accepted ZZ; approved by IEEE/ACM TRANSACTIONS ON NETWORKING Editor XY. Date of publication YZ; date of current version XZ. This research was supported by Cisco and by NSF grants CNS-1801857 and CNS-1642929. (Corresponding author: Peshal Nayak.)

P. Nayak is with the Department of Electrical and Computer Engineering, Rice University, Houston, TX, 77005 USA (e-mail: peshal.nayak@rice.edu).

M. Garetto is with the Dipartimento di Informatica, Università di Torino, 10149 Turin, Italy (e-mail: michele.garetto@unito.it).

E. W. Knightly is with the Department of Electrical and Computer Engineering, Rice University, Houston, TX 77005 USA (e-mail: knightly@rice.edu).

A preliminary version of this paper was presented at IEEE Infocom 2017.

¹Further, it would be extremely interesting to experimentally verify our findings in a real network testbed, however this effort goes beyond the modeling purposes of this paper.

²In this paper we use the term user and station interchangeably.

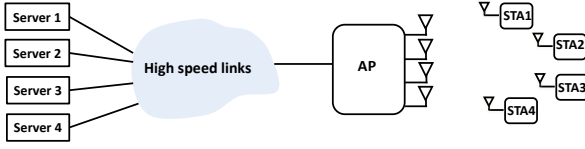


Fig. 1. Network topology for studying impact of closed loop traffic.

long-lived TCP flows to download bulk data from a set of servers located in the wired network. To isolate the targeted factors, we assume that data is sent only on the downlink, so that just TCP ACKs are sent in the uplink direction. Servers are connected to the AP over high speed links which ensures absence of congestion and queueing delays in the wired portion of the network.

In this scenario, there are no losses in the backbone, therefore each TCP flow (discarding an initial transient) operates at the maximum TCP congestion window size. As a consequence, TCP dynamics related to specific versions of the TCP protocol do not come into play in our scenario. Essentially, the only TCP feature that matters is the fact that data (ACK) packets are transmitted by TCP senders (receivers) in response to ACK (data) packets received in the opposite direction. This captures the closed-loop nature of the traffic generated by almost all versions of TCP.

Note that, while operating at the maximum congestion window size, TCP senders transmit one data packet in response to each TCP ACK (or two data packets, if the delayed ACK option is enabled [6]). We assume that all TCP flows traverse the same AP, which is equipped with multiple antennas and performs MU-MIMO transmissions on the wireless channel whenever possible, i.e., when the AP has backlogged traffic for more than one user.

As is the case with IEEE 802.11ac, uplink transmissions by the stations are instead single-user, i.e., the STAs transmit on the uplink one at a time as dictated by random access. In general, the STAs could also be equipped with multiple-antennas, and thus perform SU-MIMO by transmitting multiple streams to the AP simultaneously (we account for this in our analysis).

We will be especially interested in analysing the standard case in which channel access is governed by the fair 802.11 contention mechanism, which provides equal probability of contention victory to all nodes competing for transmission: each node that intends to transmit generates a random value for the backoff timer chosen uniformly from $[0, W_0 - 1]$ where $W_0 = 16$ is the minimum contention window size. While the channel is sensed idle, the node counts down with a slot duration of σ , and transmits when the backoff timer becomes zero.

Since the random channel access protocol of 802.11 can be responsible for severe throughput degradation of MU-MIMO under conditions that we will uncover in this paper, alternative channel access strategies will be considered later in Sec. V.

B. Background on 802.11ac compliant MU-MIMO

Here, we review the key components of the 802.11ac timeline for our analysis. When the AP obtains access to

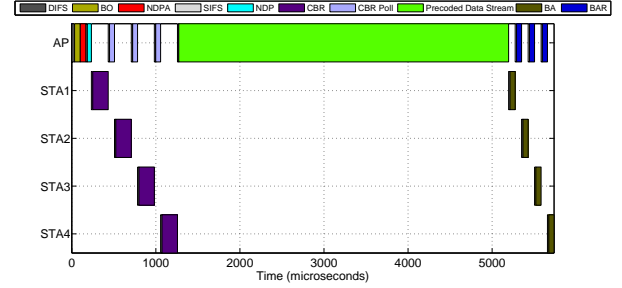


Fig. 2. An example of 802.11ac downlink transmission timeline in the case of an AP with 4 transmit antennas serving 4 single-antenna STAs.

the channel by winning contention, it performs a transmission including three main phases:

Channel Sounding and feedback phase. The AP requires channel state information at the transmitter (CSIT) to limit interference among users. Consequently, it initiates a sounding process by transmitting a Null Data Packet Announcement (NDPA) which contains information that identifies the STAs that the AP intends to transmit data to on the downlink. Following this, the AP transmits a Null Data Packet (NDP) which contains the pilot sequence that the STAs use to estimate the CSI. The STAs process the CSI to calculate the angles ϕ and ψ that are used to build the transmit weight matrix at the AP [7]. The STAs transmit these in a compressed beamforming report (CBR), as polled by AP.

Data transmission phase. Data is transmitted simultaneously to the users, typically via zero-forcing beamforming using the collected CSIT. To amortize overhead and improve performance, the AP aggregates multiple frames destined to the same STA into the same data bundle. We emphasize that 802.11ac allows up to 1 MB to be aggregated per STA.

Acknowledgement phase. After the AP transmits data, the first STA responds with a Block Acknowledge (BA). Following this, the AP subsequently transmits a block acknowledgement request (BAR) to other STAs, which then transmits their BA.

Fig. 2 shows an example 802.11ac downlink transmission for an AP with four transmit antennas serving four single-antenna STAs, in the case of channel bandwidth 20MHz, sub-carrier grouping of 4 and quantization bits for ϕ and ψ being 7 and 5 respectively. These values result in the minimum possible sounding and feedback phase duration at this bandwidth. Note that, even in this case, the total overhead due to channel sounding and feedback phases is about 1.5 milliseconds. During this interval, roughly 10 data packets of size 1 KB could be transmitted using standard SISO. Therefore, aggregation of at least a few tens of frames (among all stations) is necessary to get any performance gain from MU-MIMO with respect to traditional SISO.

To validate the results obtained in this paper, we extended the simulator ns3 [8] to incorporate detailed behavior of 802.11ac compliant MU-MIMO WLANs.

TABLE I
NOTATION

K	number of stations
F_s	Number of TCP flows for each station
W_{\max}	TCP maximum window size
T_F	TCP ACK thinning factor
D	two-way propagation delay of each flow
N_{AP}	number of antennas in the AP
N_{STA}	number of antennas in a station
B_{AP}	maximum frame aggregation by AP
B_{STA}	maximum frame aggregation by a station
$A(h, b)$	channel holding time of the AP
Λ	aggregate system throughput

III. SYSTEM MODEL

A. Assumptions and notation

The main notation used to describe the considered system is summarized in Table I. Let K be the number of stations attached to the AP, each of which is a destination of at least one long-lived TCP flow. Our goal is to compute the aggregate steady-state throughput Λ achieved by the set of all TCP flows.

In some of the scenarios that we will consider, the aggregate throughput will be limited by the TCP maximum window size W_{\max} (expressed in number of segments). In those cases, we will assume for simplicity a symmetric traffic scenario: stations establish an equal number F_s of TCP flows, and all flows experience the same two-way propagation delay D in the fixed network.

To simplify the analysis, we further assume a perfect wireless channel (without errors) and a collision-free MAC protocol.³ While these assumptions are simplifications of the real system, they enable us to capture macroscopic effects into a parsimonious analytical model. Channel errors and/or collisions could be incorporated in the analysis using well-established techniques [11], [12], but we do not do so here to keep the analysis focused on the joint impact of a closed-loop transport layer with a multi- and single-user MAC. Further, collisions typically produce only a second-order effect, while they do not lead to closed-form expressions (i.e., they require numerical fixed-point solutions).

We consider an AP implementing a work-conserving policy: when it has at least one packet to transmit, the AP starts contending for channel access. When it wins the channel, the AP employs multi-user MIMO whenever it has packets queued for at least two different stations (if it has packets destined to only a single station, the AP employs single-user MIMO). Note that the AP maintains a separate queue to store the packets destined to each attached station. Let

³Under the 802.11 MAC protocol, the absence of collisions can be obtained (i.e., simulated with ns3) by assuming that the backoff extracted by a node is continuous, rather than discrete, and that nodes instantaneously freeze their backoff as soon as another node starts transmitting.

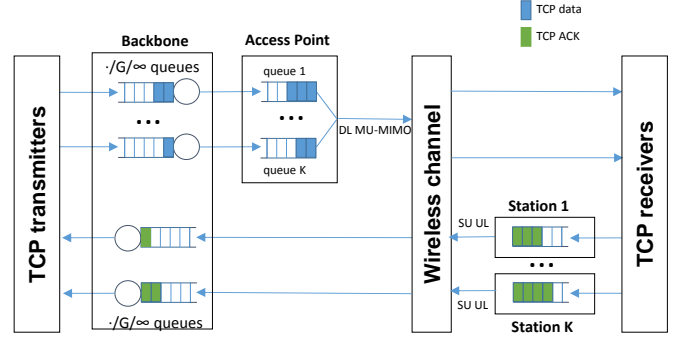


Fig. 3. Representation of the system as a closed queueing-network.

N_{AP} be the number of antennas in the AP. Let N_{STA} be the number of antennas in each of the stations. If $N_{\text{AP}} < K$, it is possible that the number of stations for which the AP has a non-zero backlog is larger than the number of antennas at the AP. In this case, we assume that the AP will pick N_{AP} different stations with non-zero backlog uniformly at random. Let $A(h, b)$ be the channel holding time of the AP, which depends on two parameters: the number of non-empty queues h , and the largest backlog b of these queues. Note that $A(h, b)$ is a known deterministic function of h and b , given physical system parameters.

Let B_{AP} be the maximum number of frames destined to the same station that can be aggregated and sent by the AP in the same channel access. Note that B_{AP} will never constrain performance when $B_{\text{AP}} > F_s W_{\max}$, since in any case the AP cannot store a number of frames destined to the same station larger than the product of the TCP maximum window size times the number of flows per station.

Let B_{STA} be the maximum number of frames (TCP ACKs, in our case) destined to the AP that can be aggregated and sent by a station in the same channel access.

We emphasize that the vast majority of existing performance evaluation studies of 802.11, focused on early versions of the standard, only consider the case $B_{\text{STA}} = B_{\text{AP}} = 1$. The impact of aggregation (in particular, possibly different levels of aggregation performed by the AP and by the stations) is instead fundamental to understand the performance of MU/SU MIMO systems.

B. High-level packet dynamics

The diagram in Fig. 3 illustrates the high-level dynamics of the system represented as a closed queueing network. The top part represents TCP data packets flowing downlink from servers to clients. The bottom part represents TCP ACKs flowing uplink from clients to servers. Recall that the AP maintains a separate queue for each of the attached stations. Based on our assumptions, one-way delays in the backbone can be modeled as infinite-server queues with deterministic service time. However, for greater generality, we describe propagation delays incurred by individual packets as i.i.d. random variables with general distribution. Consequently, we model one-way delays in the backbone as $1/G/\infty$ queues.

Consider, for now, the case in which TCP receivers send one ACK for each data packet (we relax this assumption later). Then TCP receivers essentially ‘transform’ data packets into ACKs, whereas TCP transmitters transform ACKs into data packets. Except for their different sizes, data packets and ACKs can be both considered as individual customers circulating around the network.

Since we assume that packets are never lost, each long-lived TCP flow reaches a steady-state condition with W_{\max} outstanding packets in the network. As a consequence, the system indeed behaves as a multi-class closed queueing network with a constant number of ‘customers’, where it is not really important to distinguish whether customers are data packets or TCP ACKs⁴.

Unfortunately, batch arrival/services, and more importantly the fact that wireless channel contention correlates the dynamics of MAC queues in the AP with those in the stations, do not allow us to actually solve the queueing network model with traditional techniques (such as product-form solution). Nevertheless, bottleneck analysis can still be applied to compute the long-term throughput of the system. Indeed, the aggregate system throughput Λ essentially depends on how fast the customers of the closed queueing network depicted in Fig. 3 circulate around the network.

We can view the population of customers as a fluid pushed forward by three main ‘pumps’: the downlink pump (the AP), the uplink pump (the stations), and the backbone. Correspondingly, each of the above pump has a reservoir where the fluid gets accumulated waiting to be drained. Note that the three pumps are in a specific circular order, each pushing fluid into the reservoir of the next pump in the sequence. Since the power of the three pumps is, in general, different, we can expect the fluid to be found most of the time in the reservoir of the slowest of them, which will act as the system bottleneck. The difficulty of the analysis lies in the fact that the power of the pumps depends on the amount of fluid (belonging to each flow) found on the associated reservoir. However, the maximum power of either the downlink or the uplink pump quickly reaches a saturation level as soon as enough fluid is found in their buffers. Hence we can easily determine which one of them is the strongest under the assumption that a large enough amount of fluid (for each flow) is present in their reservoirs (by comparing the saturation throughput in downlink/uplink). This will lead us to make a first distinction between two fundamental regimes: the *downlink bottleneck* case (when the maximum power of the downlink pump is smaller than the maximum power of the uplink pump) and the *uplink bottleneck* case (viceversa).

Note, however, that we will also consider cases in which this distinction is not possible, because the total amount of fluid in the system is not large enough to steadily operate at the saturation level neither in downlink nor in uplink. In these cases, the system does not have a well-defined bottleneck.

The backbone pump is somehow different because its capacity does not saturate to any value (the data rate on the

backbone is supposed to be infinite). Indeed, the impact of the backbone is just to delay the fluid in transit from the uplink pump to the downlink pump. Nevertheless, there are cases (large propagation delays) in which almost all fluid is found in the reservoir associated with the backbone (i.e., packets flying in the backbone), rather than in the other buffers of the system. Therefore, by increasing the propagation delays, we eventually reach a third regime in which the backbone becomes the main system bottleneck, despite the fact that its capacity is infinite, because of the limitation in the total amount of fluid in the system.

Consider, initially, the case in which the number of packets flying in the backbone reaches its maximum value. This case always occurs when D is very small (possibly zero), or when W_{\max} is large enough that TCP flows completely ‘fill the pipe’. Then a simple saturation throughput analysis, to be described next, allows us to understand where the rest of customers are primarily to be found (i.e., either in the AP or in the stations).

C. Saturation throughput analysis

Suppose we start from a condition in which the MAC queues of the AP, and the MAC queue of each station, have a large backlog. The AP moves packets down into the stations, while stations push up packets back into the AP (through the backbone). Who wins?

The key observation here is that contention for the wireless channel is fair among all nodes trying to transmit on it. Therefore, on average, for one downlink transmission performed by the AP, we will have K uplink transmissions performed by the set of all stations. Now, under the assumption that the AP employs multi-user MIMO (if $N_{AP} > 1$), whereas stations employ single-user MIMO, the AP will push down on average

$$S_{\text{down}} = B_{AP} \cdot \min\{N_{AP}, K \cdot N_{STA}\}$$

in each cycle of $K + 1$ transmissions. Indeed, the number of concurrent streams is given by the minimum between the number of antennas on the transmitting and receiving sides, and we can assume that the maximum allowed number of packets (equal to B_{AP}) is transmitted on each stream. During the same cycle of $K + 1$ transmissions, the stations will send up on average

$$S_{\text{up}} = K \cdot B_{STA} \cdot \min\{N_{AP}, N_{STA}\} \cdot T_F$$

effective TCP ACKs. Indeed, each station will have (on average) one opportunity to transmit B_{STA} packets using single-user MIMO, and we have accounted for the fact that TCP receivers might thin the feedback traffic to improve performance [13], by transmitting only one out of T_F (Thinning Factor) ACKs. For example, the standard delayed ACK option of TCP [6] corresponds to $T_F = 2$. For later purposes, let $S_{sta} = B_{STA} \cdot \min\{N_{AP}, N_{STA}\} \cdot T_F$ be the maximum number of (effective) TCP ACKs sent by a station in one access, so that $S_{up} = K S_{sta}$.

If $S_{\text{down}} > S_{\text{up}}$, the AP will eventually be able to move its backlog into the stations, maintaining its queues almost empty from that time on. If $S_{\text{down}} < S_{\text{up}}$, the stations will instead be able to drain their backlog, and most of the packets will be

⁴System customers are classified only by the ID of the station acting as source/destination.

found in the AP. If $S_{\text{down}} = S_{\text{up}}$, the AP and the set of all stations will maintain on average an equal backlog.

We emphasize that existing analytical models of IEEE 802.11 have focused only on the case $S_{\text{down}} \leq S_{\text{up}}$. This can be explained by the fact that, prior to the introduction of multi-user technique, it was reasonable to assume $B_{\text{STA}} = B_{\text{AP}}$ (and in many models $B_{\text{STA}} = B_{\text{AP}} = 1$), and $N_{\text{AP}} \leq K \cdot N_{\text{STA}}$. Note that earlier versions of 802.11 (without MIMO) correspond to $N_{\text{AP}} = N_{\text{STA}} = 1$. In all cases above, the AP becomes the performance bottleneck under closed-loop (e.g., TCP) traffic.

Multi-user MIMO has changed the picture by making the AP much more powerful than the typical station. Not only can the AP be equipped with many more antennas than its attached stations (which by itself would not be enough to move the bottleneck to the uplink), but more importantly, the AP must employ significant frame aggregation ($B_{\text{AP}} \gg 1$) to amortize the overhead necessary to set up multi-user transmissions. As a consequence, the performance bottleneck can shift to the uplink, which is one novel scenario analysed in our work.

D. Fundamental regimes

When there are enough packets flowing in the system to ‘fill the backbone pipe’, i.e., when the propagation delay D is small enough and, jointly, the average window size of TCP transmitters is not too small,⁵ previous discussion leads us to distinguish the following three fundamental regimes:

- **downlink bottleneck regime.** This regime occurs when both $S_{\text{down}} \leq S_{\text{up}}$ and $KF_s W_{\text{max}} \gg S_{\text{down}}$. Under the above conditions, the AP can be assumed to operate in saturation conditions, i.e., to be always fully backlogged. This is actually a desirable property to achieve the capacity gain of DL MU-MIMO.
- **uplink bottleneck regime.** This regime occurs when both $S_{\text{down}} > S_{\text{up}}$ and $F_s W_{\text{max}} \gg S_{\text{sta}}$. Under the above conditions, each station can be assumed to operate in saturation conditions, i.e., to be always fully backlogged.
- **full aggregation regime.** This regime occurs when both $S_{\text{down}} \geq KF_s W_{\text{max}}$ and $S_{\text{sta}} \geq F_s W_{\text{max}}$. Under the above conditions both the AP and the stations perform a large enough packet aggregation to completely empty their buffers at each channel access. This regime is different from the others because no node transmitting on the channel operates in saturation conditions.

Note that the *full aggregation* regime is a limiting case of the downlink (uplink) bottleneck regime as we increase the aggregation level performed by the AP (the stations).

As we increase the backbone delay D , or reduce the average window size of TCP flows, the system performance will eventually be limited by the wired network delay, rather than the wireless channel dynamics. In our analysis, we will also (partially) explore the impact of the backbone delay D in the regimes described above. In Sec. VI, we will also explore by

simulation what happens when TCP flows experience non-zero loss probability, due to buffer overflows or other reasons.

Remark. One crucial observation that we can already make at this point is the following: the size of data packets, and that of TCP ACKs, plays no role in determining the regime in which the system operates, as one can check by inspecting the conditions listed above for each regime. Specifically, the fact that TCP ACKs are much smaller in size than a TCP data packet does not modify in any way the system bottleneck. This fact is in sharp contrast to a common misconception, according to which the impact of uplink traffic is negligible because TCP ACKs are “small” (in size). As we will see, instead, the uplink feedback process can determine the overall system performance, although the large majority of traffic volume (in terms of bytes) flows downstream.

E. Reference system and basic throughput bounds

To validate our analysis we will consider a reference system closely following the network topology illustrated in Fig. 1 and the physical-layer parameters described in Sec. II-B. Specifically, we will always assume an AP equipped with 4 antennas (equal to the maximum number of concurrent streams considered in 802.11ac), operating at 54 Mb/s physical data rate per stream.

Stations are instead assumed to have a single antenna⁶, thus performing single-user SIMO transmissions in the uplink. Unless otherwise specified, we assume 4 stations in the network, so that all of them can potentially be served concurrently by the AP.

We further assume that each station establishes a single long-lived TCP flow with a server ($F_s = 1$). Unless otherwise specified, the maximum TCP congestion window size is $W_{\text{max}} = 200$. The TCP segment size is 1024 bytes, and we enable the delayed ACK option ($T_F = 2$).

In the next section, we will compare analytical results (for each of the regimes in Sec. III-D) with detailed ns3 simulations obtained in our reference system. To put our throughput figures under the right perspective, it is important to keep in mind the following simple upper bounds on Λ .

Given a physical data rate of 54 Mb/s, and 4 antennas, clearly we cannot exceed the trivial upper bound $\Lambda^{(1)} = 54 \cdot 4 = 216$ Mb/s, corresponding to the unrealistic case of zero overhead everywhere. Under the constraint of adopting the best 802.11ac-compliant MU-MIMO in the downlink, we obtain a better (tighter) bound as $\Lambda^{(2)} = KF_s W_{\text{max}} / A(K, F_s W_{\text{max}})$, by assuming zero overhead in the uplink: after the AP sends down the aggregate of all system packets, all data is acknowledged in zero time by the TCP receivers. In our reference system with $K = 4$, $F_s = 1$, $W_{\text{max}} = 200$, we obtain $\Lambda^{(2)} = 192.5$ Mb/s. At last, assuming that all system packets, after being dumped by the AP, are sequentially acked by the stations (actually, one ACK every 2 packets, since $T_F = 2$), we obtain $\Lambda^{(3)} = KF_s W_{\text{max}} / [A(K, F_s W_{\text{max}}) + T_{\text{up}}(KF_s W_{\text{max}}/2)] = 172.5$ Mb/s, where $T_{\text{up}}(KF_s W_{\text{max}}/2)$ is the channel time to send 400 TCP ACKs, in our case.

⁵So far we have assumed for simplicity a loss-free network bringing TCP sources to steadily operate at the maximum window size. However, analogous considerations can be done when the congestion window size of each flow oscillates around some (large) value due to a (small) packet loss probability.

⁶Due to size and cost constraints on mobile hand held devices, STAs tend to have fewer antennas than the AP.

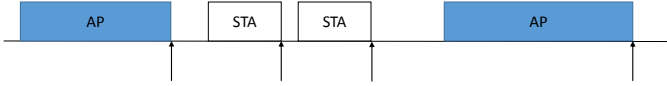


Fig. 4. Embedded discrete-time Markov Chain to analyse the downlink bottleneck regime.

IV. ANALYSIS

A. Downlink bottleneck regime

Recall that in this regime we assume the AP to be always fully backlogged. We consider a discrete-time Markov Chain embedded at the time instants at which the wireless channel becomes idle (i.e., at the end of a transmission) – see Fig. 4. The state of this Markov Chain is the set of queue lengths of the stations at the beginning of a cycle.

Standard renewal theory allows us to write the aggregate throughput Λ (in packets per seconds) as

$$\Lambda = \frac{\text{average number of packets sent in a cycle}}{\text{average cycle duration (s)}} \quad (1)$$

where packets can be *either* TCP data packets or (effective) TCP ACKs. Indeed, flow conservation (closed-loop traffic) implies that throughput in terms of data packets must be equal to throughput in terms of (effective) ACKs.

Any cycle is divided into two parts: a contention phase and a packet transmission phase. Let \hat{K} be the random variable denoting the number of contending stations at the beginning of a cycle. To simplify the analysis, we assume that random backoffs are chosen according to an exponential distribution of mean $1/\mu$, instead of a uniform distribution in $[0, W_0 - 1]$ (in number of slots of duration σ). To match the first moment of the backoff distribution, we correspondingly set $\mu = 2/(W_0\sigma)$. This way we can exploit the memoryless property of the exponential distribution and ignore the backoff time spent by a node in previous cycles. Note that this is a standard technique to simplify the analysis of 802.11, and it is known to introduce negligible errors (see [9] and Fig. 8).

It follows that the average duration of the contention phase, conditioned on having $\hat{K} = k$ contending stations ($k = 0, 1, \dots, K$), is⁷ $\frac{1}{(k+1)\mu}$. If the AP wins the contention, which occurs with probability $\frac{1}{k+1}$, we have a downlink transmission of a data bundle by the AP consisting of S_{down} TCP data packets, occupying the channel for a duration $T_{\text{down}} = A(K, B_{\text{AP}})$. Instead, with probability $\frac{k}{k+1}$ the contention is won by a station, that will occupy the channel for a duration T_{up} .

An exact analysis of the system requires to track the queue lengths of the stations. However, following this approach would be an overkill, given that the system obeys flow conservation in the downlink and uplink directions. Actually, the only advantage of performing the above exact analysis would be to perfectly characterize the duration of the contention phase at the beginning of a cycle, which has however negligible impact on the overall throughput. Therefore, we adopt the following simplifying assumptions: i) a station always transmits $\min(B_{\text{AP}}, S_{\text{sta}})$ packets when it gets access on the channel;

ii) the number \hat{K} of contending stations, which is a random variable, is replaced by a constant value k^* obtained by flow conservation:

$$\frac{1}{k^* + 1} S_{\text{down}} = \frac{k^*}{k^* + 1} \min(B_{\text{AP}}, S_{\text{sta}})$$

which provides⁸ $k^* = \frac{S_{\text{down}}}{\min(B_{\text{AP}}, S_{\text{sta}})}$. These might appear to be rough approximations but, to say it again, they only impact the computation of the average contention time at the beginning of a cycle, which has negligible impact on the throughput.

The above considerations allows us to derive the throughput according to (1):

$$\Lambda = \frac{\frac{1}{k^* + 1} S_{\text{down}}}{\frac{1}{(k^* + 1)\mu} + \frac{1}{k^* + 1} T_{\text{down}} + \frac{k^*}{k^* + 1} T_{\text{up}}} = \frac{S_{\text{down}}}{1/\mu + T_{\text{down}} + k^* T_{\text{up}}} \quad (2)$$

At last, we account for the fact that, as we increase the backbone two-way delay D , we will enter at some point the regime in which the backbone becomes the performance bottleneck. To do so, we adopt a simple approach based on the assumption that the queues of the AP are in one of two states: they are either empty, or they have sufficient backlog to send S_{down} packets in one channel access.

Let

$$\bar{C} = \frac{1}{\mu} + T_{\text{down}} + k^* T_{\text{up}}$$

be the average time to send S_{down} packets downlink (the denominator of (2)). Suppose that we start from a condition in which all $K F_s W_{\text{max}}$ packets in the system are stored in the AP. If the backbone delay is too large, the queues of the AP will not get refilled in time to maintain it constantly backlogged. In particular, the AP will run out of packets if $D > \bar{C} \frac{K F_s W_{\text{max}}}{S_{\text{down}}}$, i.e., if the backbone delay is larger than the (average) time to completely drain the AP queues. Moreover, to be sure that the AP sends S_{down} packets in each channel access, we assume that at least S_{down} packets have to be stored in its buffers: if there are not enough packets in the system to fill the pipe and guarantee enough backlog in the AP, we simply assume that the AP remains completely idle for some time. Specifically, we consider the AP to be fully backlogged for a fraction of time given by $\frac{K F_s W_{\text{max}}}{(1 + \frac{D}{\bar{C}}) S_{\text{down}}}$, if this fraction is smaller than one.

The final formula for the throughput, valid whenever $S_{\text{down}} \leq S_{\text{up}}$, $K F_s W_{\text{max}} \gg S_{\text{down}}$, becomes:

$$\Lambda = \frac{S_{\text{down}}}{1/\mu + T_{\text{down}} + k^* T_{\text{up}}} \cdot \min\left(1, \frac{K F_s W_{\text{max}}}{(1 + \frac{D}{\bar{C}}) S_{\text{down}}}\right) \quad (3)$$

Fig. 5 compares simulation results (blue, thick lines) against analytical prediction (3) (red, thin lines) in our reference system, as we vary the aggregation level employed by all nodes, for different values of backbone delay D . We do not show confidence intervals for simulation results since they are too narrow (at 95% level) to be visible.

Note that, with $B_{\text{AP}} = B_{\text{STA}}$, we are in the *downlink bottleneck* regime. As expected, the model is less accurate when D comes into play, or (for $D = 0$) when the assumption

⁸The value of k^* computed in this way is, in general, not an integer, but we do not have to worry about this.

⁷Recall that the (saturated) AP is always contending for channel access.

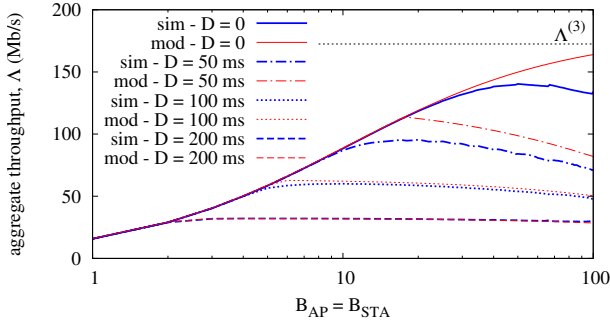


Fig. 5. Throughput comparison (model vs simulation) in the reference system, with $B_{AP} = B_{STA}$.

$KF_s W_{\max} \gg S_{\text{down}}$ (which here reads $800 \gg 4B_{AP}$) does not hold. Interestingly, there is an optimal aggregation level (strongly related to $F_s W_{\max}$) which maximizes throughput. This can be explained by the fact that, as we push B_{AP} close to $F_s W_{\max}$, we obtain diminishing returns from amortizing the overhead of setting up MU-MIMO, while increasing the probability that the AP completely empties one of its MAC queues, resulting in lower multiplexing gain. Unfortunately, such kind of optimization of the aggregation level requires knowledge of $F_s W_{\max}$, and can hardly be done in practice.

We conclude that in the *downlink bottleneck* regime the fundamental reason that can prevent achieving the theoretical performance gains of MU-MIMO is the limited amount of data packets in the queues of the AP, necessary to amortize the overhead of MU-MIMO transmissions. Such limitation, in the absence of packet losses at the transport layer⁹, is essentially related to the maximum TCP congestion window size and the number of concurrent flows for each station. In Sec. VI we will explore by simulation scenarios in which TCP flows experience losses, for example due to congestion. Of course in this case another performance factor coming into play is the packet loss probability, which can make the window size of TCP flows oscillate around too small values, causing inefficient frame aggregation by the AP.

B. Uplink bottleneck regime

Recall that in this case we assume the stations to be always fully backlogged. In this paper, we will analyze this regime under two additional assumptions¹⁰: i) the backbone delay $D = 0$; ii) the AP completely empties its queues when it gets access on the channel. Assumption i) can represent the network scenario in which servers are located within the same LAN of the stations. Assumption ii) holds in the uplink bottleneck regime when $N_{AP} \geq K$.

The main difficulty of the analysis lies in the fact that now the AP, differently from the downlink bottleneck regime, is not fully backlogged, thus it typically aggregates only a limited number of packets, which can severely degrade the maximum theoretical throughput computed under saturation conditions.

⁹Note that losses on the wireless channel due to poor channel quality are automatically recovered by the MAC protocol.

¹⁰Relaxing either of these two assumptions is analytically challenging, and we leave it to future work.

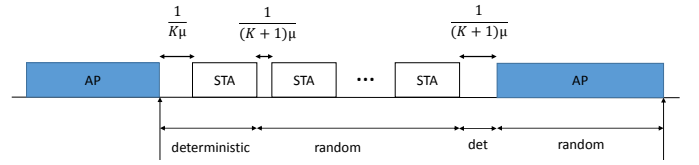


Fig. 6. Cycle analysis for the uplink bottleneck regime with $D = 0$.

Recall that the channel holding time $A(h, b)$ of the AP depends on both the number of non-empty queues h in the AP (hereinafter called user diversity) and their maximum backlog b . Let H be the random variable denoting the user diversity, and B the maximum queue length among the AP queues. Let $P(h, b) = \mathbb{P}[H = h, B = b]$ be the joint discrete distribution of the above two variables at the time instant at which the AP gets access on the channel. Note that since the AP has contended for channel access, we have $h \in \{1, \dots, K\}$, $b \in \{1, \dots, F_s W_{\max}\}$.

Suppose, for now, that $P(h, b)$ is known. In Appendix A we show how $P(h, b)$ can be analytically computed. The aggregate system throughput can then be derived by a simple cycle analysis, illustrated in Fig. 6.

This time we consider cycles delimited by time instants at which the AP releases the channel. Since the AP flushes out all its backlog, any cycle starts deterministically with a contention phase among K backlogged stations, of average duration $\frac{1}{K\mu}$, followed by the transmission of the winning station, of duration T_{up} . Now, since the backbone delay is zero, the ACKs sent up by this station will immediately create new data packet(s) in the AP, which will start contending as well. Before the AP will eventually win the contention, a random number of stations will be able to transmit. Actually, on average each station will be able to put one transmission on the channel before the AP wins. This result derives from the assumption that backoffs are exponential: by conditioning on the value x extracted by the AP, the number of transmissions made by a station is Poisson distributed of parameter μx . Deconditioning w.r.t. x , we obtain that on average each station makes one transmission before the AP, of duration T_{up} , preceded by a contention period of average duration $\frac{1}{(K+1)\mu}$.

The cycle ends deterministically with another contention period of average duration $\frac{1}{(K+1)\mu}$ (the one won by the AP) followed by the channel holding time by the AP, whose average duration is $\sum_{h,b} P(h, b)A(h, b)$. To compute the average number of packets sent in a cycle, it is convenient to express this number in ACKs, rather than data packets, since we have already shown that on average we see K transmissions by the set of all stations, plus the deterministic transmission at the beginning of the cycle.

Putting everything together, the usual renewal formula (1) provides the throughput for this scenario:

$$\Lambda = \frac{(K+1)S_{\text{sta}}}{\frac{1}{K\mu} + (K+1)\left(\frac{1}{(K+1)\mu} + T_{up}\right) + \sum_{h,b} P(h, b)A(h, b)} \quad (4)$$

To get insights into the resulting system performance, we compute here the marginal user diversity distribution $P(h) =$

$\mathbb{P}[H = h]$ through an alternative method that does not require us to first derive the joint distribution $P(h, b)$. This computation leads indeed to a rather simple and instructive result that we will discuss later on.

We first isolate the impact of the initial deterministic ACK, computing the user diversity distribution $\hat{P}(h)$ produced by stations' transmissions following the first one. By conditioning on the backoff value x extracted by the AP, we can write:

$$\hat{P}(h) = \int_0^\infty \binom{K}{h} (1 - e^{-\mu x})^h e^{-\mu x(K-h)} \mu e^{-\mu x} dx$$

Integrating by parts, we get

$$\hat{P}(h) = \int_0^\infty \binom{K}{h} \frac{h}{K-h+1} (1 - e^{-\mu x})^{h-1} e^{-(K-(h-1))\mu x} \mu e^{-\mu x} dx$$

Noticing now that $\binom{K}{h} \frac{h}{K-h+1} = \binom{K}{h-1}$, the above expression means that $\hat{P}(h) = \hat{P}(h-1)$. In other words, the distribution of $\hat{P}(h)$ is uniform over $h = 0, 1, \dots, K$, hence $\hat{P}(h) = \frac{1}{K+1}$.

To compute the distribution $P(h)$, that includes the contribution of the first ACK, we observe that $H = h$ occurs in two possible ways: i) either the first ACK belongs to one of the h queues which are already non-empty for effect of subsequent transmissions of the stations, with probability $\frac{h}{K}$, or it increases by one the number $h-1$ of non-empty queues produced by the other transmissions, with probability $\frac{K-(h-1)}{K}$. We obtain:

$$P(h) = \hat{P}(h) \frac{h}{K} + \hat{P}(h-1) \frac{K-(h-1)}{K} = \frac{1}{K}$$

meaning that $P(h)$ is also uniform over the set of possible values $h = 1, 2, \dots, K$.

This result has striking consequences on the efficiency of MU-MIMO, which strongly relies, in addition to the availability of large per-station backlog, on large user diversity (i.e. multiplexing gain). Note that the optimal operating point of MU-MIMO is full diversity ($h \geq N_{AP}$), which naturally occurs in the downlink bottleneck regime.

In the uplink bottleneck regime, instead, wireless channel contention can result into a random user-diversity far from the optimal one. Under the scenario considered in this section ($K \leq N_{AP}$), the average user diversity is $(K+1)/2 \leq K$, which results roughly into a throughput reduction by factor $(K+1)/(2K)$, which in our reference system (with $K = 4$) equals $5/8 = 0.625$. Note that the penalty introduced by such sub-optimal user-diversity is intrinsic to the random access nature of the channel, and thus unavoidable (in the uplink bottleneck regime). Instead, the penalty due to small per-station backoff can be eliminated by letting the stations perform packet aggregation in a way similar to what the AP does.

Throughput formula (4) can be refined for the case in which the number S_{sta} of effective ACKs sent by a station in one channel access is so large that assumption $F_s W_{max} \gg S_{sta}$ no longer holds (but notice that we still assume $S_{down} > S_{up}$, so that the system operates in the uplink bottleneck regime). In particular, we can refine the analysis under the assumption that $F_s W_{max} = \bar{m} S_{sta}$, where $\bar{m} \geq 1$ is an integer. In words, we assume for simplicity that the total number of packets

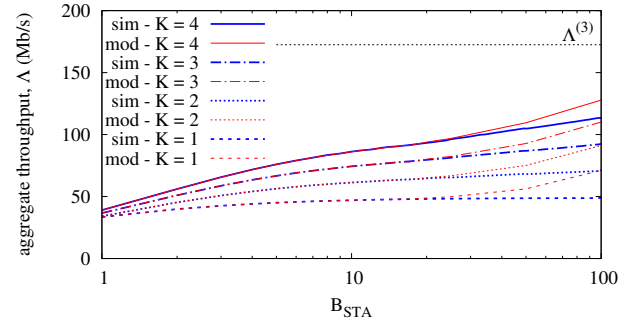


Fig. 7. Throughput comparison (model vs simulation) in the reference system, with $B_{AP} = \infty$, $D = 0$, as function of B_{STA} , for different number of stations.

belonging to a station is a multiple of S_{sta} . In this case, a station cannot clearly transmits more than \bar{m} times in a cycle. To account for this fact, we need to derive the distribution $P(m) = \mathbb{P}[M = m]$ ($0 \leq m \leq \bar{m}$) of the r.v. M denoting the number of transmissions performed by a station while contending with the AP, before the AP wins the contention.

By conditioning on the backoff value x extracted by the AP, we can write:

$$P(m) = \int_0^\infty \frac{(\mu x)^m}{m!} e^{-\mu x} \mu e^{-\mu x} dx = \frac{1}{2^{m+1}}$$

As expected, if the station could make an arbitrarily large number of transmissions ($\bar{m} = \infty$), we would get the average value:

$$\mathbb{E}[M] = \sum_{m=0}^{\infty} \frac{m}{2^{m+1}} = 1$$

When M cannot exceed the maximum value \bar{m} we get instead:

$$\mathbb{E}[M] = \sum_{m=0}^{\bar{m}-1} \frac{m}{2^{m+1}} + \sum_{m=\bar{m}}^{\infty} \frac{\bar{m}}{2^{m+1}} = \frac{2^{\bar{m}} - 1}{2^{\bar{m}}}$$

which provides the improved throughput formula:

$$\Lambda = \frac{\left(1 + \frac{2^{\bar{m}} - 1}{2^{\bar{m}}}\right) S_{sta}}{\frac{1}{K\mu} + (K+1) \left(\frac{1}{(K+1)\mu} + T_{up}\right) + \sum_{h,b} P(h,b) \bar{A}(h,b)} \quad (5)$$

where $\bar{A}(h,b) = A(h, \min\{b, F_s W_{max}\})$ takes again into account the fact that the number of packets sent by the AP, belonging to the same station, cannot exceed $F_s W_{max}$.

Fig. 7 compares the analytical prediction (5) against simulation in our reference system (with $D = 0$), as we vary the aggregation level B_{STA} employed by stations. Here we assume unlimited aggregation by the AP (actually, $B_{AP} \geq F_s W_{max}$), bringing to system to operate in the *uplink bottleneck* regime. As expected, the model is less accurate when the assumption $F_s W_{max} \gg S_{sta}$ (which here reads $200 \gg 2B_{STA}$) does not hold.

Focusing on the basic case $K = 4$, we observe severe throughput loss when B_{STA} is small, due to poor frame aggregation by the AP.¹¹ But even with unlimited aggregation by the stations (actually, the maximum level of aggregation by stations is already achieved with $B_{STA} = 100$) the throughput is

¹¹without the delayed ACK option, with $B_{STA} = 1$ we would get $\Lambda = 23.9$ Mb/s, smaller than that of a DL SU system! (see Sec. V).

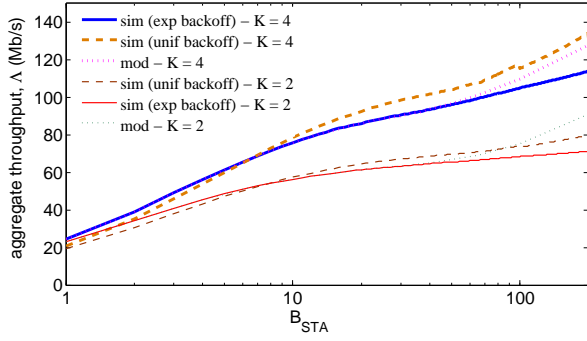


Fig. 8. Throughput comparison (model vs simulation) in the reference system, with $B_{AP} = \infty$, $D = 0$, as function of B_{STA} , for $T_F = 1$, $K = 2$ or $K = 4$.

only about 113 Mb/s¹², which is $0.65 \cdot \Lambda^{(3)}$ (see Sec. III-E), close to our analytical prediction of a throughput reduction by factor $\frac{K+1}{2K} = 0.625$.

Impact of backbone delay. See our Supplemental Material for a simulation investigation on the impact of backbone delay in the uplink bottleneck regime.

Impact of backoff distribution. Our analysis is based on the simplifying assumption that the random backoff chosen by each station contending for channel access is taken from an exponential distribution, rather than the actual uniform (discrete) distribution dictated by the 802.11 standard. Indeed, the uniform distribution would not allow us to make the simple cycle analysis illustrated in Fig. 6, since cycles would no longer be independent of each others. On the other hand, the error introduced by such simplifying assumption is expected to be of secondary importance, as already observed in many 802.11 models, under both saturated and unsaturated conditions [9], [10]. For this reason, and to better highlight the impact of the other simplifying assumptions introduced in our analysis, we have preferred to adopt an exponential backoff distribution also in our simulations.

For completeness, we report here a comparison of results obtained under the uniform vs exponential backoff distribution, for the scenario already considered in Fig. 7. However, to avoid repetition of results, this time we disable the delayed ACK TCP option, i.e., we consider $T_F = 1$. Results shown in Fig. 8 confirm the second-order effect due to the shape of the backoff distribution. They also show that, by disabling the delayed ACK option, we obtain worse performance, especially for small levels of aggregation performed by stations (for $B_{STA} = 1$, the throughput is only slightly larger than 20 Mb/s, whereas it was around 40 Mb/s with $T_F = 2$, see Fig. 7).

C. Full aggregation regime

Recall that in this case both the AP and the stations perform a large enough packet aggregation to completely empty their buffers at each channel access. Since the current 802.11 standards allow to adopt large levels of aggregation (around

1 MB), possibly larger than the TCP maximum window size, we believe this regime to be quite important in practice.

The main effect produced by large aggregation performed by both AP and stations is the following: all packets circulating in the system, and associated to the same station (under our assumptions, $F_s W_{\max}$ packets) cluster together and move as a single entity (a large batch) across the network. Note that this phenomenon does not depend on initial conditions nor on the value of backbone delay.

The above behavior allows us to develop a simpler analytical model than that in Sec. IV-B, accounting also for backbone delay. We start analyzing the case of $D = 0$. We adopt the same cycle analysis illustrated in Fig. 6. This time, however, we can have at most one transmission by each station in between two consecutive transmissions by the AP. Actually, we can directly exploit the computation of $P(h)$ done in Sec. IV-B, and conclude that the number of transmissions performed by stations in a cycle has the uniform distribution over $1, \dots, K$. Let T_{up} be the time required by a station to send $F_s W_{\max}$ (effective) ACKs in the uplink. The usual renewal formula (1) provides in this case:

$$\Lambda = \frac{\sum_{h=1}^K \frac{1}{K} h F_s W_{\max}}{\frac{1}{\mu K} + \sum_{h=1}^K \frac{1}{K} \left(A(h, F_s W_{\max}) + h T_{up} + \sum_{j=0}^{h-1} \frac{1}{\mu(K-j)} \right)} \quad (6)$$

Let us now consider a scenario in which the backbone delay is extremely small, but larger than the maximum channel contention time (i.e., slightly larger than $W_0 \sigma$). It happens here that the last batch of ACKs sent up by a station in a cycle cannot arrive at the AP in time to be immediately resent down in the following AP transmission (marking the end of the current cycle). Therefore, this last batch will be aggregated with those sent by the AP at the end of the next cycle. One important consequence of this fact is that, with non-zero delay, we never see the maximum value ($h = K$) of user diversity. This explains the sharp initial drop that we observe in the throughput as we step out of $D = 0$ (see Fig. 9).

Specifically, with small delay the distribution of user diversity becomes:

$$P(h) = \begin{cases} \frac{2}{K} & h = 1 \\ \frac{1}{K} & 2 \leq h \leq K-1 \end{cases} \quad (7)$$

whose average value is $\frac{K^2 - K + 2}{2K}$. Indeed, the AP only contends with $K - 1$ stations during a cycle, after receiving the last batch sent up in the previous cycle. These $K - 1$ stations send a number of batches uniformly distributed in $[0, K - 1]$, but the last of them (if any) cannot be transmitted in the same cycle. On the other hand, we need to add the last batch sent in the previous cycle. Similarly, if stations do not send any batch during a cycle, the AP will start contending after receiving one batch, again with $K - 1$ stations.

The corresponding throughput formula can be concisely written as:

$$\Lambda = \frac{\sum_{h=0}^{K-1} \frac{1}{K} \max(1, h) F_s W_{\max}}{\sum_{h=0}^{K-1} \frac{1}{K} \left(A(\max(1, h), F_s W_{\max}) + h T_{up} + \sum_{j=0}^h \frac{1}{\mu(K-j)} \right)} \quad (8)$$

leading to a throughput reduction roughly equal to $\frac{K^2 - K + 2}{2K^2}$.

¹²This value requires exactly $D = 0$. Under more realistic conditions of small but not null delay, we would get $\Lambda = 86$ Mb/s, see Sec. IV-C.

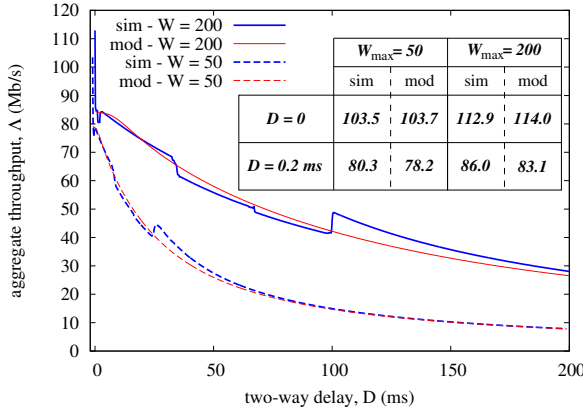


Fig. 9. Throughput comparison (model vs simulation) in the reference system, under the full aggregation regime ($B_{AP} \geq W_{\max}$, $B_{STA} \geq W_{\max}$), for $W_{\max} = 50$ or 200 , as function of backbone delay D .

To compute the throughput in the case of larger delays, we adopt a useful approximation which consists of assuming that the network delay D is exponentially distributed (instead of deterministic). Such approximation greatly simplifies the analysis, while providing an accurate throughput prediction. Indeed, the memoryless property of the exponential distribution allows us to embed a discrete-time Markov Chain at the boundaries of the cycles as in Fig. 6, with a bi-dimensional state (m_1, m_2) denoting (assuming $K > 1$): the number $1 \leq m_1 < K$ of batches transmitted by the AP at the end of previous cycle (recall that this number cannot be equal to K , with non-zero delay); the number $0 \leq m_2 \leq K - m_1$ of batches stored by the stations. Then the remaining batches $m_3 = K - m_1 - m_2$ are still ‘flying’ in the backbone, with remaining time to arrive at the AP exponentially distributed with mean D . Note that the total number of states, equal to $\frac{K^2+K-2}{2}$, is typically small (in the order of K^2).

We can easily express the transition probabilities among the above defined states, and use the stationary distribution of the Markov Chain in (1) (details can be found in App. B).

Fig. 9 compares analytical predictions obtained by our Markov Chain model against simulation as we vary the backbone delay D , for two different values of TCP maximum window size $W_{\max} = 50$ or 200 . We observe that the analytical predictions (based on the exponential delay assumption) nicely interpolate the rather complex curves obtained from simulation under deterministic delay.

The table inserted on the plot also shows the accuracy of (6) (for $D = 0$) and (8) (for small but non null delay). Results for the latter (more realistic) case of non-null delay confirms that no more than 86 Mb/s can be achieved by full aggregation in the reference system with $W_{\max} = 200$, which is 50% of bound $\Lambda^{(3)} = 172.5$ Mb/s, as roughly predicted by factor $\frac{K^2-K+2}{2K^2}$, equal to 44%, with $K = 4$.

V. COMPARISON OF UPLINK STRATEGIES

Since the traditional random access mechanism of 802.11 does not allow us to fully exploit the capacity gain of downlink MU-MIMO under closed-loop traffic, we may ask which

alternative schemes (specifically intended for the uplink traffic) could be used to improve the throughput.

We will again focus on our reference system (under the best case $D = 0$), for which theoretical throughput bounds have been already computed in Sec. III-E.

A simple solution to avoid the performance degradation inherent to random channel access is to make the uplink operate under the AP’s coordination. Consider, for example, a simple polling mechanism working as follows: right after transmitting down a data bundle, the AP polls each station to which it has transmitted data to send up a corresponding number of packets. Clearly, this scheme allows to achieve bound $\Lambda^{(3)} = 172.5$ Mb/s.

Note that upper bound $\Lambda^{(2)} = 192.5$ could be approached in a similar way, if stations were also able to send up a single (small) cumulative ack for all data received from the AP. This could actually be obtained at the transport layer by increasing the thinning factor T_F . Note, however, that massive use of delayed ACK techniques (beyond the standard $T_F = 2$) has detrimental effects to TCP [13], and would require sophisticated cross-layer design to be implemented in a WLAN.

At last, we could employ multi-user transmissions also in the uplink (as is expected to be the case with the upcoming 802.11ax). In particular, consider a vanilla MU uplink with zero overhead¹³, that allows backlogged stations to aggregate and concurrently send up many packets (TCP ACKs, in our case) in the uplink. Even employing the standard delayed ACK option ($T_F = 2$), such scheme would achieve, with full aggregation, throughput as high as $\Lambda^{(4)} = KF_s W_{\max} / [A(K, F_s W_{\max}) + T_{up}(F_s W_{\max}/2)] = 187.0$ Mb/s, where $T_{up}(F_s W_{\max}/2)$ is the channel time to send 100 TCP ACKs, in our case.

Fig. 10 visually compares the throughputs achieved in several interesting cases that we have analyzed and discussed so far, in our reference system (always with unlimited aggregation by the AP). The first bar shows that, in the case of $B_{STA} = 1$, $T_F = 1$, the throughput that we get by using SU DL is actually larger than what we get by enabling MU DL (second bar)! The third bar (related to the full aggregation regime) shows the huge throughput loss (around 50%) intrinsically due to random channel contention. The last two bars are related to the alternative uplink strategies discussed in this section.

VI. IMPACT OF PACKET LOSSES

To simplify the analysis and capture the key performance factors into a parsimonious model, we have assumed so far that packets are never lost/corrupted in the network, allowing TCP flows to reach their maximum congestion window size. Specifically, TCP flows do not experience losses because we have considered a scenario in which: i) the capacity of the wired portion of the network is overprovisioned; ii) the

¹³Similar to DL MU-MIMO, a multi-user uplink transmission also requires some overhead to set up communication [22]. While a multi-user uplink is yet to be standardized in the upcoming 802.11ax standards, prior works such as [23] have demonstrated schemes to reduce this uplink overhead to as little as 100 μ s which is approximately 10 times less as compared to the sounding overhead for DL MU-MIMO.

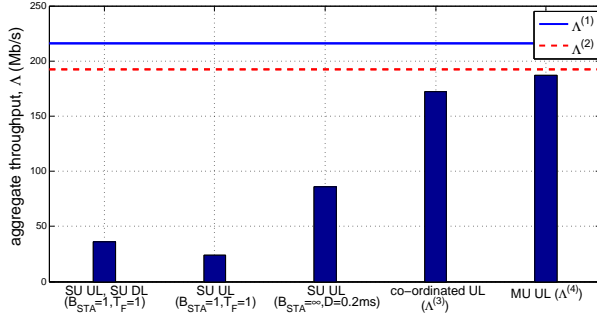


Fig. 10. Comparison of throughputs achieved in the reference system, with $D = 0$, $B_{AP} = \infty$, under different settings and access strategies.

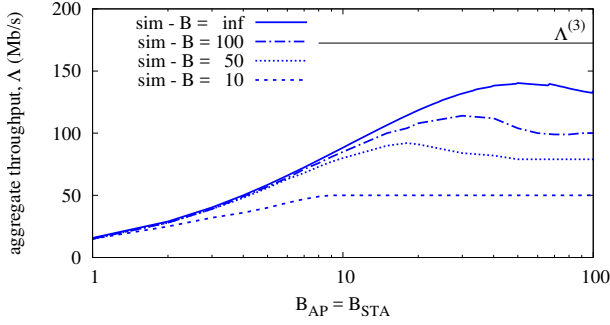


Fig. 11. Impact of finite buffer size at the AP, in the downlink bottleneck regime with $B_{AP} = B_{STA}$.

AP/STAs can buffer unlimited amount of data for each flow; iii) the wireless channel is error-free. What happens when the above assumptions do not hold?

We can expect that factors preventing MU-MIMO from achieving its maximum capacity gains under ideal conditions (i.e., in the absence of losses) persist also under non-ideal conditions (i.e., in the presence of losses), leading to even worse throughput. Here, we explore this issue in exemplary scenarios as follows, for both the downlink and uplink bottleneck regime.

Fig. 11 shows TCP throughput obtained by simulation in the reference scenario with $K = 4$ stations, $D = 0$, under the downlink bottleneck regime (the analogous of Fig. 5). We assume now that the AP can buffer a finite number B of data packets for each flow, and consider $B = 100, 50, 10$. Here, TCP flows suffer from losses due to buffer overflow at the AP, limiting their congestion window size as dictated by the congestion control algorithm (in our case, NewReno). Since aggregation of a number of data frames larger than the buffer size is impossible, curves flatten for $B_{AP} \geq B$. A small overshoot is observed when B_{AP} approaches B from below.

Fig. 12 shows TCP throughput obtained by simulation in the reference scenario with $K = 4$ stations, $D = 0$, under the same MAC and physical-layer assumptions considered in Fig. 7, where we observed, in the absence of losses, the onset of the uplink bottleneck regime. We now ask whether the presence of losses can cause the network to not enter the uplink bottleneck regime. The answer to this question is in the affirmative since, by increasing the loss probability we make TCP flows operate at smaller and smaller window sizes,

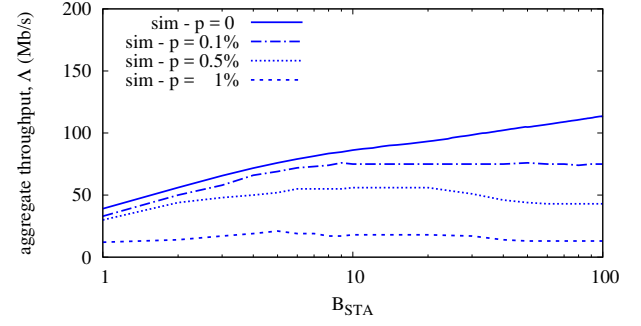


Fig. 12. Throughput obtained by simulation in the reference system, with $B_{AP} = \infty$, $D = 0$, $K = 4$ as function of B_{STA} , for different values of packet loss probability.

eventually leading to the condition in which station queues are no longer saturated, and performance gets limited by TCP dynamics, rather than by wireless channel dynamics. In this respect, the (poor) throughput obtained in the absence of losses (when we get into the uplink bottleneck regime), acts as an upper bound to the throughput achievable with the addition of losses.

To show this fact, we introduce an artificial (Bernoulli) loss probability p in the downlink, which could model non-ideal conditions due to i) congestion in the wired network, ii) residual errors on the wireless channel not automatically recovered by the MAC protocol.

With loss probability 0.1%, we obtain a curve similar to that obtained in the uplink bottleneck regime (achieved under zero losses). We also observe that increasing the aggregation size at the STA beyond about 10 does not provide any benefit, which can be explained by the fact that frame aggregation performed at the STAs gets limited by the TCP window size. Higher loss probabilities lead to further throughput reductions: when TCP flows operate at too small window size, MAC-layer dynamics are no longer the bottleneck (actually we are no longer in the uplink bottleneck regime), and overall performance is essentially determined by TCP dynamics in response to losses and end-to-end delay.

VII. RELATED WORK

The capacity gain of MU-MIMO has been widely investigated at the PHY layer, considering various schemes to acquire CSI and different precoding techniques to enable simultaneous data transmission (e.g., [14], [15]). However, the impact of traffic dynamics on the achievable throughput performance is still not well understood.

Novel hardware design, measurement and performance evaluation of MU-MIMO has been presented in works such as [16], [17], [18]. While such works confirm the capacity gains expected from MU-MIMO, their focus remains entirely on the PHY and channel related performance parameters. Consequently, these gains are evaluated under scenarios wherein the AP is always fully backlogged. This is orthogonal to our research which focuses on cross-layer analysis of MU-MIMO WLANs operating under closed loop (TCP) dynamics.

MAC protocols [19], [20] that exploit the higher transmission capabilities of the advanced MU-MIMO PHY layer have

been designed and evaluated with over-the-air experiments. In [21] authors propose a queueing model for MU-MIMO under open loop (non-saturated) traffic. Various user scheduling algorithms for poor channel quality avoidance are analyzed in [24]. However, crucial assumptions made in the papers above is that the AP is always fully backlogged, or that traffic is open loop only.

There exists a huge body of literature on modeling 802.11 (i.e., variations of [11]), considering also the impact of closed-loop traffic (TCP) (e.g., [12]). However, to the best of our knowledge, no work has explored so far the performance of MU-MIMO under closed-loop traffic and 802.11 contention.

VIII. CONCLUSION

We presented the first cross-layer analysis of a random access WLAN where DL MU-MIMO is coupled with a SU uplink, considering the impact of closed-loop (TCP) traffic. Despite the fact that the majority of traffic volume flows downlink, our analysis revealed the emergence of a dichotomy between a downlink bottleneck regime and an uplink bottleneck regime, depending on several parameters such as the number of stations/antennas, frame aggregation levels, and thinning of feedback traffic. With the help of our analytical models, we identified crucial performance factors that offset the gains achievable by DL MU-MIMO, showing the intrinsic limitations due to random channel contention. We have also taken a system design view discussing strategies to mitigate this loss and allow MU-MIMO WLANs to achieve their theoretical capacity under closed loop traffic.

APPENDIX A

COMPUTATION OF JOINT DISTRIBUTION $P(h, b)$

We can limit ourselves to the case in which stations send just one effective TCP ACK in each channel access ($S_{\text{sta}} = 1$). The extension to the case in which stations send $S_{\text{sta}} > 1$ effective ACKs in each channel access is trivial, since it just requires to scale the distribution obtained for $S_{\text{sta}} = 1$ accordingly.

To obtain an exact expression of $P(h, b)$ in the case of zero-delay backbone, we separately account for the impact of the initial deterministic ACK at the beginning of a cycle (see Fig. 6). So, let us first consider the distribution produced by uplink transmissions following the first one. For them, we actually compute the more detailed joint pdf $\hat{P}(h_1, h_2, b)$ where: b is the maximum queue length; $h_1 \geq 1$ is the number of queues having exactly length b ; $h_2 \geq 0$ is the number of queues having length strictly less than b . By conditioning on the backoff value x extracted by the AP, we can write:

$$\hat{P}(h_1, h_2, b) = \int_0^\infty \binom{K}{h_1} \left[\frac{(\mu x)^b}{b!} e^{-\mu x} \right]^{h_1} \cdot \binom{K-h_1}{h_2} \left(\sum_{j=1}^{b-1} \frac{(\mu x)^j}{j!} e^{-\mu x} \right)^{h_2} e^{-\mu x(K-h_1-h_2)} \mu e^{-\mu x} dx \quad (9)$$

Despite their ugly look, integrals of the form (9) have a closed-form expression, obtained by expanding them into a sum of contributions, each leading to an analytical solution. Just as an example, in the case of $K = 4$,

$$\hat{P}(2, 1, 3) = \binom{4}{2} \binom{2}{1} \frac{1}{(3!)^2} \left(\frac{7!}{1! 5^8} + \frac{8!}{2! 5^9} \right) = \frac{3024}{390625}$$

Note that $\hat{P}(h_1, h_2, b)$ are some ‘universal’ numbers that depend only on K , and that can be computed once and for all and made available through, e.g., a table lookup.

To derive the final joint pdf $P(h, b)$ we have to add the contribution of the first deterministic ACK:

$$P(h, b) = \sum_{h_1+h_2=h-1} P(h_1, h_2, b) \frac{K-h+1}{K} + \sum_{h_1+h_2=h} P(h_1, h_2, b-1) \frac{h_1}{K} + \sum_{h_1+h_2=h} P(h_1, h_2, b) \frac{h_2}{K} \quad (10)$$

In the above expression, the first summation corresponds to the case in which the first ACK increases the user-diversity (and not b); the second summation corresponds to the case in which the first ACK does not increase the user-diversity (but it increases b); the third summation corresponds to the case in which the first ACK does not increase neither the user-diversity nor b .

APPENDIX B

FULL AGGREGATION CASE WITH NON-NEGLIGIBLE DELAY

We compute the transition probabilities of the Markov Chain by considering the number of batches that can arrive from the backbone between two consecutive transmissions by the AP, and the fact that the AP, if it receives at least one batch, will transmit again after a number of transmissions by the stations uniformly distributed in $0, 1, \dots, m_1 + m_2$.

Let $p_{[m_1, m_2 \rightarrow m'_1, m'_2]}$ denote the transition probability from state (m_1, m_2) to state (m'_1, m'_2) . To avoid unnecessary complications, we assume that batches flying in the backbone, in number $m_3 = K - m_1 - m_2$, can arrive at the AP during an interval of duration

$$V(m_1, m_2) = T(m_1, F_s W_{\text{max}}) + \sum_{j=1}^{m_1+m_2} \left(\frac{1}{\mu j} + T_{\text{up}} \right)$$

comprising the AP transmission at the end of previous cycle plus the time required by stations to send up all of their batches by competing only among themselves. Let $\lambda = 1/D$ be the arrival rate of a batch from the backbone. With probability $e^{-\lambda m_3 V}$ no batch arrives, and we get the (set of) transitions

$$p_{[m_1, m_2 \rightarrow 1, 0]} = e^{-\lambda(K-m_1-m_2)V(m_1, m_2)} \quad (11)$$

The reason for transiting to state $(1, 0)$ is that, eventually, one batch will arrive at the AP, while all of the others will be still flying in the backbone.

With probability

$$\rho(k, m_1, m_2) = \binom{m_3}{k} (1 - e^{-\lambda V})^k e^{-\lambda(m_3-k)V}$$

we have, instead, k batch arrivals during V ($1 \leq k \leq m_3$). Assuming for simplicity that all these arrivals occur before nodes start to contend again on the channel, the AP will transmit the above k batches after a number of transmissions by the stations uniformly distributed in $0, \dots, m_1 + m_2$, leading to the transition probability:

$$p_{[m_1, m_2 \rightarrow k, m_1+m_2-j]} = \frac{\rho(k, m_1, m_2)}{m_1 + m_2 + 1} \quad 0 \leq j \leq m_1 + m_2$$

Note that one of these transitions, specifically the one with $k = 1$, $j = m_1 + m_2$, should be added (i.e., contribute) to the one introduced before in (11) (we have preferred to split the two contributions, with abuse of notation, for better readability).

With the above transition probabilities, one can then solve the Markov Chain and obtain the stationary probability distribution π_{m_1, m_2} .

It remains to explain how this distribution can be used to compute the numerator and the denominator of throughput formula (1). The numerator (average number of packets sent in a cycle) is simply:

$$\sum_{m_1, m_2} \pi_{m_1, m_2} m_1 F_s W_{\max}$$

The denominator (average cycle duration) can be expressed instead as an average ‘reward’ over all possible transitions:

$$\sum_{m_1, m_2, m'_1, m'_2} \pi_{m_1, m_2} \cdot P_{[m_1, m_2 \rightarrow m'_1, m'_2]} \cdot r(m_1, m_2, m'_1, m'_2)$$

where $r(m_1, m_2, m'_1, m'_2)$ is the reward associated to the transition from state (m_1, m_2) to state (m'_1, m'_2) . Hence, we only need to specify the rewards associated to the possible state transitions. The reward associated to the zero arrival transition (11) is $V(m_1, m_2) + \frac{D}{K} + \frac{1}{\mu}$. Indeed, after the interval of duration V all batches will be flying in the backbone, and the first will arrive on average D/K later, and will be sent by the AP after an average backoff $1/\mu$.

The reward associated to the transition with probability $P_{[m_1, m_2 \rightarrow k, m_1 + m_2 - j]}$ instead, is equal to

$$T(m_1, F_s W_{\max}) + \sum_{i=0}^j \frac{1}{\mu(m_1 + m_2 + 1 - i)} + jT_{up}$$

since, after the transmission by the AP, we have j transmissions by the stations, each preceded by a contention phase of proper average duration.

REFERENCES

- [1] IEEE 802.11ac/D7.0, “Enhancements for Very High Throughput for Operation in Bands Below 6 GHz,” 2013.
- [2] O. Bejarano, et al., “IEEE 802.11ac: from channelization to multi-user MIMO,” *IEEE Communications Magazine*, vol. 51, no. 10, pg. 84-90, 2013.
- [3] D. Murray and T. Koziniec, “The state of enterprise network traffic in 2012,” *In Proc. of IEEE APCC*, 2012.
- [4] J. L. Garcia-Dorado, et al., “Characterization of ISP Traffic: Trends, User Habits, and Access Technology Impact,” *IEEE Trans. on Network and Service Management*, 9(2), pg. 142–155, 2012.
- [5] A.K. Marnerides, et al., “Internet traffic characterisation: Third-order statistics & higher-order spectra for precise traffic modelling,” *Computer Networks*, Volume 134, pp. 183–201, 2018.
- [6] R. Braden, “RFC-1122: Requirements for internet hosts,” *Request for Comments*, pg. 356-363, 1989.
- [7] E. Perahia, and R. Stacey, “Next Generation Wireless LANS: 802.11n and 802.11ac,” *Cambridge university press*, 2013.
- [8] ns3, <https://www.nsnam.org/>, Accessed: 2016-07-28.
- [9] F. Calì, M. Conti, E. Gregori, “Dynamic Tuning of the IEEE 802.11 Protocol to Achieve a Theoretical Throughput Limit,” *IEEE/ACM Trans. Netw.*, 8(6), pg. 785–799, 2000.
- [10] M. Garetto and C.F. Chiasserini, “Performance Analysis of 802.11 WLANs Under Sporadic Traffic,” *In Proc. of IFIP Networking*, 2005.
- [11] G. Bianchi, “Performance Analysis of the IEEE 802.11 Distributed Coordination Function,” *IEEE JSAC*, 18(3), pg. 535–547, 2006.

- [12] A. Kumar, et al., “New Insights from a Fixed-point Analysis of Single Cell IEEE 802.11 WLANs,” *IEEE/ACM Trans. Netw.*, 15(3), pg. 588–601, 2007.
- [13] D. Miorandi, et al., “A Queueing Model for HTTP Traffic over IEEE 802.11 WLANs,” *Computer Networks*, 50(1), pg. 63–79, 2006.
- [14] T. Yoo and A. Goldsmith, “On the optimality of multi-antenna broadcast scheduling using zero-forcing beamforming,” *IEEE JSAC*, 24(3), pg. 528–541, 2006.
- [15] G. Caire, et al., “Multiuser MIMO achievable rates with downlink training and channel state feedback,” *IEEE Trans. on Inf. Theory*, 56(6), pg. 2845–2866, 2010.
- [16] N. Anand, et al., “The case for UHF-band MU-MIMO,” *In Proc. of ACM MobiCom*, 2014.
- [17] K. Shepard, et al., “Argos: Practical many-antenna base stations,” *In Proc. of ACM MobiCom*, 2012.
- [18] E. Aryafar, et al., “Design and Experimental Evaluation of Multi-user Beamforming in Wireless LANs,” *In Proc. of ACM MobiCom*, 2010.
- [19] N. Anand, et al., “Mode and user selection for multi-user MIMO WLANs without CSI,” *In Proc. of IEEE INFOCOM*, 2015.
- [20] O. Bejarano, et al., “MUTE: sounding inhibition for MU-MIMO WLANs,” *In Proc. of IEEE SECON*, 2014.
- [21] B. Bellalta, et al., “An approximate queueing model for multi-rate multi-user MIMO systems,” *IEEE Communications Letters*, 15(4), pg. 392–394, 2011.
- [22] K. Tan, et al., “SAM: enabling practical spatial multiple access in wireless LAN,” *In Proc. of ACM Mobicom*, 2009.
- [23] A. Flores, et al., “A Scalable Multi-User Uplink for Wi-Fi,” *In Proc. of USENIX NSDI*, 2016.
- [24] C. Chen and L. Wang, “Performance Analysis of Scheduling in Multiuser MIMO Systems with Zero-Forcing Receivers,” *IEEE JSAC*, 25(7), pg. 1435–1445, 2007.



Peshal Nayak is a Ph.D. candidate in the Department of Electrical and Computer Engineering at Rice University in Houston, Texas, USA. He received the M.S. degree in Electrical and Computer Engineering from Rice University and the B.Tech. degree in Electrical Engineering from the Indian Institute of Technology Patna. His research interests are in experimental wireless networking, testbed design, cross layer protocol design, mathematical modeling and performance evaluation. He was a recipient of the Texas Instruments Distinguished Student Fellowship and Best-In-Session presentation award at IEEE INFOCOM 2017.



Michele Garetto (M'04) received the Dr.Ing. degree in Telecommunication Engineering and the Ph.D. degree in Electronic and Telecommunication Engineering, both from Politecnico di Torino, Italy, in 2000 and 2004, respectively. In 2002, he was a visiting scholar with the Networks Group of the University of Massachusetts, Amherst, and in 2004 he held a postdoctoral position at the ECE department of Rice University, Houston. He is currently associate professor at the University of Torino, Italy.



Edward W. Knightly (S'92–M'96–SM'04–F'09) received the B.S. degree from Auburn University, and the M.S. and Ph.D. degrees from the University of California at Berkeley. He is currently the Sheafor-Lindsay Professor and the Chair of the Department of Electrical and Computer Engineering, Rice University. His research interests are in experimental wireless networking, urban-scale testbeds, 60-GHz, -THz, and VLC bands, wireless security, and performance evaluation. He is a Sloan Fellow. He was a recipient of the NSF CAREER Award and Awards from ACM MobiCom, ACM MobiHoc, and IEEE SECON.

has received Best Paper Awards from ACM MobiCom, ACM MobiHoc, and IEEE SECON.

Supplemental Material

IMPACT OF BACKBONE DELAY IN THE UPLINK BOTTLENECK REGIME

Here we investigate by simulation what happens in the uplink bottleneck regime when the backbone delay D is not zero. Quite surprisingly, we observed in simulation that backbone delay has a beneficial impact on the aggregate throughput, which exhibits an intriguing non-monotonic behavior: it first increases with the delay (though with diminishing returns, i.e., through a concave function), up to a maximum value reached for $D = D^*$, after which it decreases to zero following a convex function, resulting into a ‘fin’ shape – see Fig. 14 (top plot).

Puzzled by this fact, we investigated simulation traces discovering the origin of this behavior. We considered our reference system, in the case in which stations do not perform any packet aggregation ($B_{STA} = 1$) or feedback traffic thinning ($T_F = 1$).

Fig. 13 shows a simulation trace for the total number of packets sent by the AP in each channel access, for the particular delay value $D = 120$ ms. It can be clearly recognized a cycle-stationary behavior of duration slightly smaller than 200 ms. In the following, we will call ‘super-cycle’ each cycle of this roughly-periodic behavior. A ‘super-cycle’ is internally structured in two phases: a first phase in which the AP sends just a few packets (< 10) in each channel access (*pump* phase), and a second phase in which the AP sends many more packets in each channel access (*drain* phase). The roughly periodic behavior illustrated in Fig. 13 shows up for any value of delay (except for very small delays, say smaller than 5 ms), though with a different period of duration roughly proportional to D itself (traces not shown here).

We performed a post-processing of traces like that in Fig. 13, obtaining the super-cycle first-order statistics shown in the bottom plot of Fig. 14 (note that the x axes of the top and bottom plots of Fig. 14 are aligned). In particular, we obtained the (average) total number of packets sent by the AP in each super-cycle (solid curve), and the (average) super-cycle duration (dotted curve). We clearly see that the point $D^* \approx 80$ ms at which the aggregate throughput reaches its maximum value corresponds to the point at which the total number of packets sent by the AP in a super-cycle saturates to the total number of packets circulating in the system (4 TCP flows with $W_{max} = 200 \Rightarrow 800$ packets).

To convey the physical interpretation of this behavior, suppose to start from an ideal condition in which all packets circulating in the system are all initially stored in the stations. The stations will then contend only among themselves, ‘pumping’ their packets into the backbone through a quite regular stream. If $D > D^*$, stations will actually exhaust at some point all of their backlog, and at this point all packets of the system will be ‘flying’ in the backbone. When the front of the stream generated by the stations arrives at the AP, the AP will start to contend, sending initially a small number of packets in the first channel access (possibly just one). But soon a multiplicative effect occurs: while the AP transmits on the channel, the stream arriving from the backbone (note that this

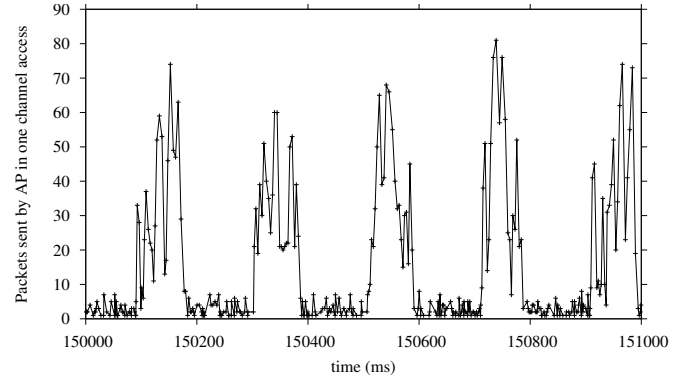


Fig. 13. Simulation trace of the number of packets sent by the AP in one channel access. Parameters as in Fig. 14.

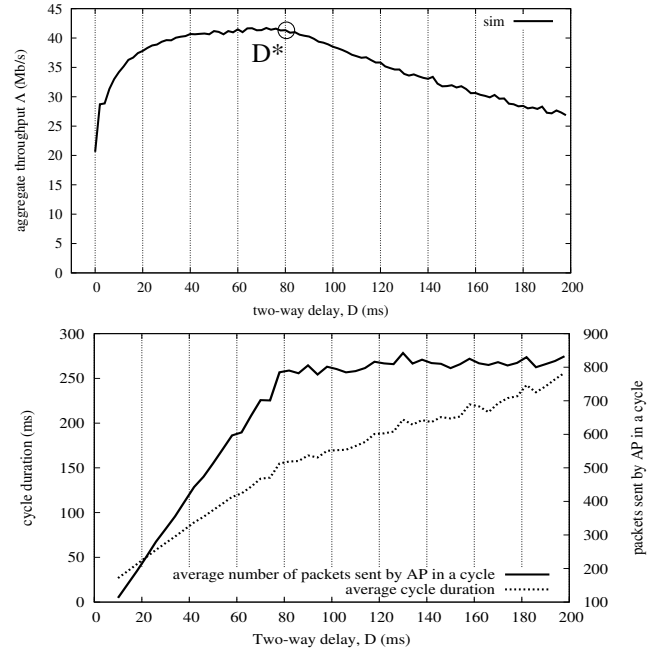


Fig. 14. Simulation results obtained in the reference system with $B_{AP} \geq W_{max}$, $B_{STA} = 1$, $T_F = 1$. Aggregate throughput (top plot), and corresponding super-cycle statistics (bottom plot).

stream is not interrupted by the fact that the channel is busy) refills the AP with many more packets to send in the next channel access (note that the intensity of the backbone stream is large enough to produce the amplification effect, since ACKs are small and the backbone capacity is large – a phenomenon sometimes referred to in the literature as ACK compression), generating a sequence of elementary cycles with increasing duration and packet aggregation. As a consequence, the AP will be able to quickly drain the backlog arriving from the backbone down again into the stations, marking the end of the super-cycle (and the beginning of a new super-cycle starting with a new pump phase). Interestingly, this pump-and-drain behavior occurs also when we do not start from the condition in which all system packets are in the stations. Moreover, the same behavior occurs when $D < D^*$.

We observed that the pump-and-drain phenomenon is strongly non-linear and highly sensitive to system parameters.

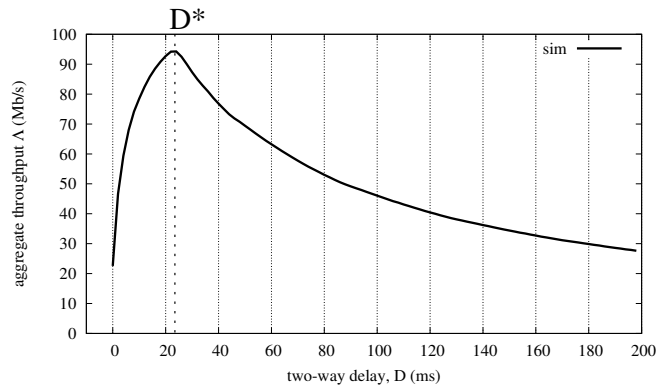


Fig. 15. Aggregate throughput obtained in the reference scenario with $B_{AP} \geq W_{\max}$, $B_{STA} = 1$, $T_F = 1$, assuming DIFS = 1 slot.

For example, by reducing the DIFS parameter of 802.11 to the slot size ($9 \mu s$), we observed a fin shape surprisingly sharper than the one in Fig. 14 (top plot), going up to 95 Mb/s! (see Fig. 15). Unfortunately, capturing such effects into a parsimonious analytical model proved to be particularly difficult.